X-616-69-143
PREPRINT

TANGENTIAL DISCONTINUITIES IN THE SOLAR WIND

L. F. BURLAGA
N. F. NESS

APRIL 1969

GODDARD SPACE FLIGHT CENTER
GREENBELT, MARYLAND

X-616-69-143

TANGENTIAL DISCONTINUITIES IN THE SOLAR WIND

L. F. Burlaga
N. F. Ness

Laboratory for Space Sciences
NASA-Goddard Space Flight Center
Greenbelt, Maryland

April 1969

Extraterrestrial Physics Branch Preprint Series

TANGENTIAL DISCONTINUITIES IN THE SOLAR WIND

Leonard F. Burlaga
and
Norman F. Ness

Laboratory for Space Sciences
NASA-Goddard Space Flight Center
Greenbelt, Maryland

Abstract

This paper considers six discontinuity surfaces which were observed by magnetometers on 3 spacecraft in the solar wind. It is shown that the actual surface orientations, determined from the measured time delays and solar wind speed, are consistent with the theoretical orientations which were computed from the relation $\hat{n}=\hat{B}\times\hat{B}'$, where $\hat{n}$ is the normal to the surface of a hydromagnetic tangential discontinuity across which the magnetic field direction changes from $\hat{B}$ to $\hat{B}'$. The plasma and magnetic field data for these discontinuities are consistent with the pressure balance condition, and the magnetic field vectors in the associated current sheets are parallel to the discontinuity surface, as required theoretically.

The 6 discontinuity surfaces extended without much distortion over ~.002 AU. A seventh surface is discussed which satisfies the condition $\hat{n}=\hat{B}\times\hat{B}'$ but which extended without much distortion over 0.02 AU. This latter is not a typical surface, however, and its curvature is larger than average. Most of the surfaces tended to lie along the spiral direction, but one was nearly perpendicular to the spiral direction.

I. Introduction

Several authors have shown that there are discontinuities in the solar wind which satisfy one or more necessary conditions for a hydromagnetic tangential discontinuity. The pressure balance and stability conditions for such discontinuities were examined by Burlaga (1968, 1969b); Fairfield (1968) showed that the mean speed of motion of such discontinuities in the magnetosheath is equal to the solar wind speed, hence they are being convected out from the sun by the solar wind. The relation between the change in the wind velocity at a discontinuity and the corresponding change in the magnetic field direction was considered by Siscoe et al. (1969). The relation between current sheets and rotational fans associated with "discontinuities" in the magnetic field direction was studied by Siscoe et al. (1968).

This note considers another necessary condition for a hydromagnetic tangential discontinuity, namely, that the normal to the surface is given by

$$\hat{n} = \hat{B} \times \hat{B}' \qquad (1)$$

where $\hat{B}$ and $\hat{B}'$ are the magnetic field directions on the two sides of the discontinuity (see Figure 1). Specifically, we shall use observations of six discontinuity surfaces, each of which was seen by three spacecraft (Explorers 33, 34, 35), to show that the orientations of the discontinuity surfaces obtained by triangulation agree with the theoretical orientations given by (1). Other necessary conditions for a tangential discontinuity are also considered. A discontinuity which was seen at Pioneer 6 and IMP-3 and discussed by Ness (1966) is re-examined in Section V.

II. Instruments, Orbits, and Selection of Discontinuities

Instruments. The magnetic field experiments on Explorers 33, 34 and 35 have been described respectively by Behannon (1967), Fairfield (1969) and Ness et al. (1967). The solar wind speeds which are used below are those measured by the plasma probe of Ogilvie and Wilkerson on Explorer 34. The plasma analyzer is described by Ogilvie et al. (1968) and a brief description of the data reduction procedure is given by Burlaga et al. (1968).

Orbits. The trajectories of Explorers 33, 34 and 35 for the period of interest in the discussion below are given in a report by Behannon et al. (1968). Explorers 33 and 34 were placed into orbit in July 1966 and May 1967 around the earth with initial apogees 72 R_E and 33 R_E, respectively. Explorer 35 was injected into a captured lunar orbit in July 1967 with aposelene 5.4 R_M. The separations between the spacecraft ranged from <10 R_E to ~ 135 R_E (100 $R_E \sim .00425$ AU). Simultaneous interplanetary data from 3 spacecraft are available from May to December 1967. Each spacecraft spends only a fraction of its orbit in the solar wind. From the figures of Behannon et al. (1968) we find that the solar wind was seen simultaneously by all 3 spacecraft $\sim$25% of the time in the period July 19, 1967 to December 13, 1967.

Selection of Discontinuities. The principal objective of this research is to demonstrate the existence of structures in the solar wind which satisfy the necessary conditions for a hydromagnetic tangential discontinuity. No attempt has been made to perform a

statistical study on all of the interplanetary discontinuities which were seen by the 3 spacecraft. In the period July 19, 1967 - December 13, 1967 all discontinuities were examined, but only 6 discontinuity surfaces were selected for this study. The 6 surfaces were chosen because the corresponding measured and calculated parameters could be determined quite accurately. Each of the selected discontinuities was identified as a change in the magnetic field direction which occurred in $\lesssim$ 1 minute and for which the angular orientation changed by 30° to $\sim 100^{\circ}$. The variations in the magnetic field were small in the 20 minute interval centered at each of the selected discontinuities. The error in the measured magnetic field intensity was $\lesssim$ 7% in most cases and the magnetic field direction was determined with $\pm$ 5^{c} in most cases. Discontinuities for which $\hat{n} = \hat{B}x\hat{B}'$ was nearly perpendicular to the earth-sun line were not accepted for this study on the grounds that if they were tangential such an orientation would imply that the discontinuity surfaces were seen nearly edge-on. The solar wind speed at the time each of the discontinuity surfaces passed Explorer 34 was measured with an error < 3%.

III. Orientations of the Discontinuity Surfaces

We shall identify the 6 discontinuity surfaces which are the principal subject of this paper by the letters A, B, C, D, E, and F. Each of these surfaces was observed by magnetometers at 3 points in space which we label (X_i, Y_i, Z_i), $i = 1,2,3$. The subscripts are chosen such that $t_1 > t_2 > t_3$ where t_i is the time that the surface passed (X_i, Y_i, Z_i). The coordinates are chosen such that $\hat{X}$ points toward the sun, $\hat{Z}$ points to the north ecliptic pole and $\hat{Y}$ completes the right-handed coordinate system.

Since each of the discontinuity surfaces was seen as a sudden change in the direction of the magnetic field at each of the three satellites, three "normals" could be computed for each surface, $\hat{n}_i = \hat{B}_i \times \hat{B}'_i$, $i = 1,2,3$. For most of the surfaces A to E the angle between $\hat{B}_i$ and $\hat{B}'_i$ was near 90°. If the discontinuity surfaces were planar over distances equal to the satellite separations ($\sim$.002 AU), the normals $\hat{n}_i$, $i = 1,2,3$, would be parallel. However, most of the discontinuity surfaces are slightly curved. The extent of the curvature can be seen in Figure 2, which shows (a) the points at which each discontinuity was observed and (b) a line segment at each point i which represents the intersection between a plane normal to $\hat{n}_i$ and the plane of the ecliptic. The curvature is relatively small (partly because of the choice of discontinuities) so each theoretical discontinuity surface can be approximated by a plane with the theoretical normal.

$$\hat{n}_T = \frac{1}{3} \sum_{i=1}^{3} \hat{n}_i = \frac{1}{3} \sum_{i=1}^{3} \hat{B}_i \times \hat{B}'_i \qquad (2)$$

The values of $\hat{n}_T$ for A to E are shown in Table I. The error limits give the extreme values of $\hat{n}_i$ observed for each surface. The sign of $\hat{n}_T$ was chosen so that it points in the sunward direction. The solar ecliptic coordinates of $\hat{n}_T$ are shown in Table II.

The orientation of a discontinuity surface can also be determined by triangulation using the three satellite observations separated in space and time. Assume that (1) each discontinuity surface can be approximated by a plane P over the distance .002 AU, (2) P moves with the solar wind speed u along the earth-sun-line, so that $V_p = -u\hat{X}$, and (3) the orientation and speed of P does not change in the interval t_3-t_1. Then at t_1 the following three points are on P: $P_1 = (X_1, Y_1, Z_1)$, $P_2 = (X_2 + ut_{12}, Y_2, Z_2)$, and $P_3 = (X_3 + ut_{13}, Y_3, Z_3)$, where $t_{1i} = t_i - t_1$. Let $\underset{\sim}{P}_1$, $\underset{\sim}{P}_2$ and $\underset{\sim}{P}_3$ be vectors from the origin to each of these points, and let the normal to P be $\hat{n}_p$. Note that the vectors $\underset{\sim}{P}_{12}=\underset{\sim}{P}_2-\underset{\sim}{P}_1$ and $\underset{\sim}{P}_{13}=\underset{\sim}{P}_3-\underset{\sim}{P}_1$ lie in P and are perpendicular to $\hat{n}_p$: If $\underset{\sim}{P}_{12}$ and $\underset{\sim}{P}_{13}$ are not parallel, then $\hat{n}_p = \hat{P}_{12}x\hat{P}_{13}$, where $\hat{P}_{12}$ and $\hat{P}_{13}$ are the unit vectors corresponding to $\underset{\sim}{P}_{12}$ and $\underset{\sim}{P}_{13}$. It happens that $\hat{P}_{12}$ and $\hat{P}_{13}$ are nearly colinear for A, B, C, and D (see Table I), so a cross product would give a large uncertainty in $\hat{n}_p$. It is still true, however, that $\hat{P}_{12}$ and $\hat{P}_{13}$ must be perpendicular to $\hat{n}_T$, the normal to the discontinuity as determined from the magnetic field observations alone, if the discontinuities are tangential. In other words, for the discontinuities to be tangential, the following necessary conditions must be satisfied:

$$\cos \alpha_{12} \equiv \hat{P}_{12} \cdot \hat{n}_T = 0 \quad \alpha_{12} = 90^\circ$$
$$\cos \alpha_{13} \equiv \hat{P}_{13} \cdot \hat{n}_T = 0 \quad \alpha_{13} = 90^\circ \qquad (3)$$

Table I shows the values of $\hat{P}_{12}$ and $\hat{P}_{13}$ which were computed for discontinuities A to F using the satellite positions shown in Figure 2, the time delays shown in Table I, and the solar wind speed u measured at the time that the discontinuities passed Explorer 34. Putting $\hat{P}_{12}$, $\hat{P}_{13}$ and $\hat{n}_T$ from Table I into (3), gives the results shown in Table II. The values of $\Delta\alpha$ in Table II represent the errors in α_{12} and α_{13}; they were computed from the errors in $\hat{n}_T$ and the less significant errors in t_i.

Table II gives the principal result of this paper: the observed orientations of each of the 6 directional discontinuities agree (within $\approx 10^\circ$) with the theoretical orientations which were calculated from (2) on the assumption that the discontinuities are tangential. In other words, the vectors $\hat{P}_{12}$ and $\hat{P}_{13}$ are perpendicular to $\hat{n}_T$, within the uncertainities of measurement, as required by (3).

This implies that the line segments at the points in each panel in Figure 2 represent intersections of a discontinuity surface with the ecliptic plane. Note that most of the surfaces in Figure 2 tend to lie along the spiral direction. This is to be expected, since the surfaces were associated with directional discontinuities and Siscoe et al. (1968), Burlaga and Ness (1968) and Burlaga (1969a) showed that on the average the theoretical surfaces associated with directional discontinuities tend to lie along the spiral direction.

Figure 2, panel E, shows a surface which is nearly perpendicular

to the spiral direction. Since the spiral direction is a macroscale concept based on long-term averages whereas discontinuities are microscale features, it is not surprising that individual discontinuity surfaces can have diverse orientations. However, this can be very significant in comparing multiple satellite data, since the time that a discontinuity spends in transit between two satellites depends strongly on the orientation of the discontinuity surface relative to the vector between the two satellite positions. In fact, using only the wind speed u, one cannot even predict which spacecraft will be the first to see a given discontinuity, given only the positions of the spacecraft (compare D and E in Figure 2).

Since the validity of the above results depends on 3 assumptions, we shall now examine the assumptions in detail.

1. The assumption of planarity is a principal source of error and is more important for some discontinuities than for others. Examination of the normals $\hat{n}_i$, i = 1,2,3 for each surface shows that the orientations of A, B and D varied $<20^\circ$ over distances $\sim 75\ R_E$, indicating that a plane is a good approximation for these surfaces. Table 2 shows that for A, B, and D, $\bar{\alpha} = 90^\circ \pm 3^\circ$ which is in good agreement with the theoretical value. The orientations of E and F varied $\sim 35^\circ$ over 85 R_E, indicating a significant curvature. For E and F, Table 2 gives $\bar{\alpha} = 91^\circ \pm 6^\circ$, indicating agreement with theory, but with a larger uncertainty. Figure 2 shows a very pronounced curvature of surface C, and examination of the normals shows that the orientation varied by $\sim 45^\circ$ over 80 R_E. Correspondingly, Table 2 shows that C is the surface for which the observed α's

differ most from 90^{o}.

2. The assumption that the surfaces move with the velocity $\vec{v} = -u\hat{X}$ implies that they are carried with the solar wind and that they move radially away from the sun. The neglect of fluctuations in the solar wind direction and of aberration does not introduce a significant error in the wind speed because the deviation is probably $<8^{o}$ and the corresponding uncertainty in the speed is only 1%. Because of the curvature of the surfaces, the uncertainties in their orientations, and the timing errors, it is very difficult to directly measure propagation speeds $\lesssim$ 50 km/sec. If the surfaces were propagating at such speeds, i.e. less than the Alfven speed, it would not appreciably change the results in Table 2 since this would correspond to $\Delta u/u \approx 10\%$, which is on the order of the errors in $\hat{n}$ and t_{ij}. On the other hand, there are no known hydromagnetic discontinuities except shocks, which propagate faster than the Alfven speed, and surfaces A to E do not have shock signatures (see Section IV). Thus, there is no theoretical reason to expect that they are moving faster than $\sim$ 50 km/sec. with respect to the solar wind. Fairfield (1968) has presented experimental evidence that directional discontinuities move with the solar wind speed. We conclude that there is no reason to believe that the assumption of essentially no propagation will introduce an appreciable error in the calculation of α.

3. We assume that the surfaces move with the fluid and that the orientation of the discontinuity surfaces does not change in the interval $t_3 - t_1$. This is equivalent to assuming that the solar

wind speed does not change in this interval and is uniform over the region defined by the positions of the three spacecraft. With only one plasma probe, it is impossible to determine $\partial u/\partial t$ or ∇u, but the order of magnitude of the changes in u can be estimated from the observed u(t). The observations show that the wind speed was lower than average and was not changing in the periods when A, B, and E were detected. This is consistent with the planarity of these surfaces, and rules out local velocity gradients as the cause of the unusual orientation of E. When D was passing the spacecraft the solar wind speed was decreasing at the rate of ~(.25 km/sec)/min. which corresponds to an insignificant change of ~ 3 km/sec. during the measurement period. There was an even smaller decrease in u in the interval when F was studied. On the day that C was detected, the wind speed was high (~550 km/sec.) and increasing, but the speed did not change significantly in the interval t_3-t_1. We conclude that the assumption of constant and uniform wind speed is probably a good approximation over the intervals of interest.

IV. Current Sheets Associated with the Discontinuities

The magnetic field change across a tangential discontinuity is maintained by a thin current sheet (see Siscoe et al. (1968) for a discussion of the theory and some observations.) The magnetic field vector should appear to rotate in the current sheet as it is convected past the observer (Burlaga 1969b). Theoretically, this rotation is in a plane parallel to the discontinuity surface, so that the individual vectors, $\underset{\sim}{B}_r$, in the current sheet should be perpendicular to $\hat{n} = \hat{B}x\hat{B}'$. In this section, we use high-resolution magnetic field data from Explorer 34 (vector measurements at 2.56 sec. intervals) to examine the structure of the current sheets associated with A to F above.

Consider the discontinuity A. The high-resolution data show that the transition from $\underset{\sim}{B}$ to $\underset{\sim}{B}'$ occurred in an interval of 10 sec. Using the measured solar wind speed (324 km/sec.) and the calculated normal, we find that this time implies the passage of a current sheet whose thickness was 3×10^{8} cm = 2×10^{-5} AU. Four measurements of the field $\underset{\sim}{B}_r$ in the current sheet were obtained during its passage. Table 3 shows that the transition from $\underset{\sim}{B}$ to $\underset{\sim}{B}'$ occurred by means of an apparently uniform rotation of the magnetic field. Furthermore, the average normal component of these vectors, the magnetic field vectors in the current sheet, were perpendicular to the normal $\hat{n} = \hat{B}x\hat{B}'$ which implies that

$$\frac{1}{4}\sum_{r=1}^{4} \underset{\sim}{B}_r \cdot \hat{n}, \text{ was } (.05 \pm .1)\gamma .$$

Similar results were obtained for the current sheets associated

with B, C, D and F. The current sheet for E was too thin to be studied. These results are summarized in Table III. The implication of these results is that the structure of the current sheets associated with A, B, C, D, and F is consistent with that which should be observed for tangential discontinuities.

V. Pressure Balance Across the Discontinuities

If the surfaces A to F do indeed represent tangential discontinuities, one should find that the pressure $B^2/(8\pi) + nk(T_p+T_e)$ is the same on both sides of each surface (here B is the magnetic field intensity, n the proton density, T_p the proton temperature, and T_e the electron temperature). This cannot be verified directly because measurements of T_e are not available but it can be tested if some assumption is made concerning the electron temperature. There was no significant change in n, B, and T_p across A, B, D, and E, so the pressure did not change across these surfaces if T_e remained constant. Across C, there was a change in n and B, but not in T_p; the density increased discontinuously from $7.8 \pm .9 cm^{-3}$ to $10.1 \pm .8 cm^{-3}$, B decreased from 14.9γ to 12.3γ, and T_p remained constant at $(400 \pm 50) \times 10^3 {}^oK$.

Using these values, we find that pressure was balanced across C if $T_e = 1.2T_p$ near that discontinuity; somewhat larger values of T_e/T_p are also allowed by the errors in n, B and T. The temperature T_p was not accurately determined near F, so the pressure balance equation cannot be verified quantitatively for this discontinuity. Qualitatively, there was an increase in the magnetic field pressure across F which was at least partly compensated by an increase in the particle pressure due to an increase in density.

VI. Remarks on an Early Multiple-Satellite Observation

Three years ago, Ness (1966) published observations of a directional discontinuity that was seen at two spacecraft, Pioneer 6 and IMP 3, which were separated by 0.009 AU. He showed that the observed transit time from Pioneer 6 to IMP 3 (57.5 minutes) was nearly the time required for an Archemedean spiral line corresponding to a 410 km/sec. wind speed to corotate from Pioneer 6 to IMP 3 (53 minutes). In effect, this showed that the orientation of the discontinuity surface (assumed to be nearly a plane) was consistent with its being along the theoretical spiral direction. If we go one step further and ask what orientation is implied by the change in the magnetic field direction, assuming that it was a tangential discontinuity, we find that this orientation was along the theoretical spiral direction (using $\hat{n} = \hat{B}x\hat{B}'$ we find that the normal has the direction $\varphi_n \approx 45^\circ$, $\theta_n \approx 25^\circ$). In other words, the observed orientation determined by Ness is consistent with that predicted by the relation $\hat{n} = \hat{B}x\hat{B}'$ for a tangential discontinuity. The alignment along the spiral direction in this case was somewhat fortuitous. Large deviations from the spiral direction can occur, as may be seen in Figure 2.

Two other points concerning this discontinuity deserve mention. First, as noted by Ness, the discontinuity extended without much distortion over nearly .01 AU. This is probably an exceptional case, due in part to the unusually quiet conditions at the time it was observed, but it suggests that surfaces of tangential discontinuities can extend over distances several times .01 AU. The second point is

that this discontinuity was discussed by Burlaga (1968) in a very different context. He showed that there was a significant, discontinuous increase in the bulk speed at the time of the directional discontinuity which was followed by oscillations in the magnetic field intensity, and that the directional discontinuity was associated with a decrease in the magnetic field intensity which was characteristic of a D sheet (Burlaga and Ness, 1968).

VII. Summary

Several necessary conditions must be satisfied for a hydromagnetic tangential discontinuity: 1) it does not propagate relative to the solar wind, 2) the magnetic fields on either side of the surface are parallel to the surface, i.e. the surface normal is given by equation (1) in the text, 3) the total pressure does not change across the surface, and 4) the magnetic field vectors in the associated current sheet are parallel to the discontinuity surface. All of these conditions must be shown to be satisfied in order to positively identify a hydromagnetic tangential discontinuity. Although conditions 1), 3) and 4) have been considered separately in previous publications, they have not been studied collectively for a single discontinuity. Condition 2) has not been previously examined at all.

This paper carries the study of tangential discontinuities one-step further by using high quality and high-time resolution interplanetary magnetic field data from three satellites and simultaneous plasma data from one of these satellites to examine the physical properties of 6 discontinuities in the solar wind. On the assumption that the discontinuities did not propagate relative to the solar wind, it was shown that the orientations of these surfaces were consistent with the theoretical orientations implied by condition 2). In other words, this paper presents discontinuities for which the equation $\hat{n} = \hat{B}x\hat{B}'$ is satisfied. The magnetic field and plasma data for these discontinuities are consistent with the pressure balance condition for a tangential

discontinuity, if the electron temperature was proportional to the proton temperature near the discontinuities. The current sheets associated with 5 of the discontinuities observed by Explorer 34 were wide enough to be studied, and it was found that in each case the structure was consistent with condition 4). Thus, the observations relating to the 6 discontinuities are consistent with all of the conditions listed above for a hydromagnetic tangential discontinuity.

It was found that the discontinuity surfaces tend to be aligned along the theoretical spiral direction, but may depart significantly from this direction in individual cases. The data in Figure 2 indicate that the discontinuity surfaces may bend noticably on a scale of .002 AU. In fact, the average curvature is undoubtedly greater than that suggested by Figure 2, since we have attempted to select the most nearly planar surfaces. On the other hand, we have discussed one surface examined earlier by Ness (1966) whose orientation was consistent with the condition $\hat{n} = \hat{B}x\hat{B}'$ and which was nearly planar over a distance of $\approx$.02 AU.

FIGURE CAPTIONS

Figure 1. The plane in this figure represents the surface of a tangential discontinuity, called P in the text. This shows that the vectors on both sides of the surface must be parallel to the surface, but their magnitude and orientations may differ.

Figure 2. Each panel summarizes the observations of one of the discontinuity surfaces A to F. The origin of the coordinates is at the earth, the scales show distances in earth radii, and $\hat{X}$ points toward the sun. Each point represents a satellite position at the time discontinuity surface passed that satellite. The points are numbered in time sequence, i.e. the surface first passed 1, then 2 and finally 3. The line segment at each point shows the ecliptic plane intersection of a plane normal to $\hat{n} = \hat{B}x\hat{B}'$, where $\hat{B}$ and $\hat{B}'$ are the directions of the magnetic field vectors measured just before and just after the surface passed the point.

REFERENCES

Behannon, K. W.: 1967, "Mapping of the Earth's Bow Shock and Magnetic Tail", J. Geophys. Res. 73, 907.

Behannon, K. W., Fairfield, D. H., and Ness, N. F.: 1968, "Trajectories of Explorers 33, 34 and 35, July 1966-July 1968", NASA-GSFC report X-616-68-372.

Burlaga, L. F.: 1968, "Micro-Scale Structures in the Interplanetary Medium", Solar Physics 4, 67-92.

Burlaga, L. F.: 1969a, "Directional Discontinuities in the Interplanetary Magnetic Field, Solar Physics, in press.

Burlaga, L. F.: 1969b, "Large Velocity Discontinuities in the Solar Wind", Solar Physics, in press.

Burlaga, L. F., Ogilvie, K. W.: 1968, "Observations of the Magnetosheath-Solar Wind Boundary", J. Geophys. Res. 73, 6167-6178.

Burlaga, L. F., and Ness N. F.: 1968, "Macro-and-Micro-Structure of the Interplanetary Magnetic Field", Canadian Journal of Physics 46, S962.

Fairfield, D. H.: 1968, "Simultaneous Measurements of Three Satellites and the Observation of the Geomagnetic Tail at $1000R_E$", J. Geophys. Res. 73, 6179-6187.

Fairfield, D. H.: 1969, "Bow Shock Associated Waves Observed in the Far Upstream Interplanetary Medium", NASA-GSFC Preprint X-616-68-454.

Ness, N. F.: 1966, "Simultaneous Measurements of the Interplanetary Magnetic Field", J. Geophys. Res. 71, 3319-3324.

Ness, N. F., Behannon, K. W., Scearce, C. S., and Cantarano, S. C.: 1967, "Early Results from the Magnetic Field Experiment on Lunar Explorer 33", J. Geophys. Res. 72, 5769.

Ogilvie, K. W., McIlwraith, N., and Wilkerson, T. D.: 1968, A Mass-Energy Analyzer for Space Plasmas", Rev. Sci. Instr., 39, 441.

Siscoe, G. L., Davis, L. Jr., Coleman, P. J., Jr., Smith, E. J., and Jones, D. E.: 1968, "Power Spectra and Discontinuities in the Interplanetary Magnetic Field: Mariner 4", J. Geophys. Res. 73, 61-68.

Siscoe, G. L., Turner, J. M., and Lazarus, A. J.: 1969, "Simultaneous Plasma and Magnetic Field Measurements of Probable Tangential Discontinuities in the Solar Wind", Solar Physics, in press.

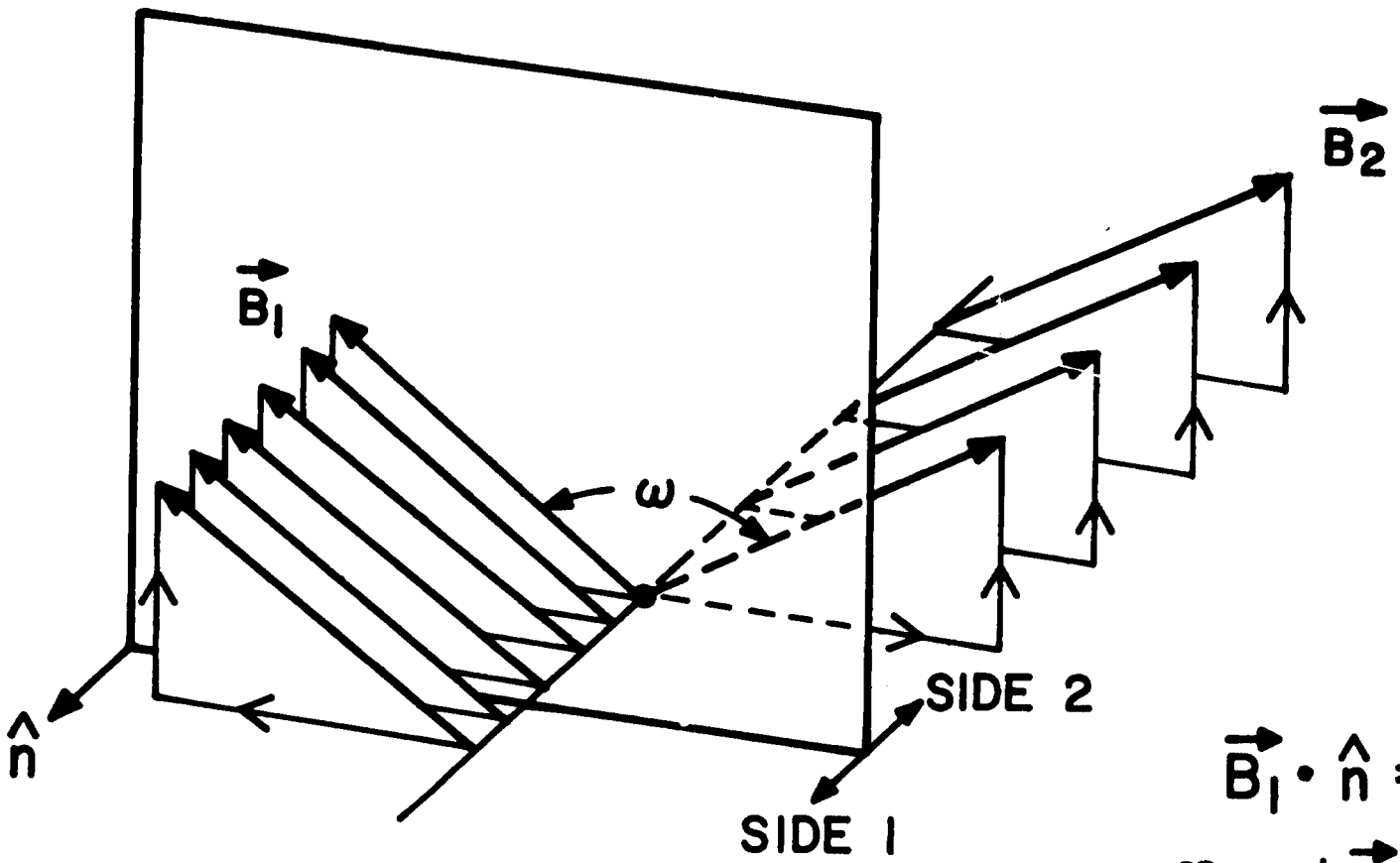

$$\vec{B}_1 \cdot \hat{n} = \vec{B}_2 \cdot \hat{n} = 0$$

$$\infty > |\vec{B}_1| / |\vec{B}_2| > 0$$

TANGENTIAL DISCONTINUITY

Figure 1

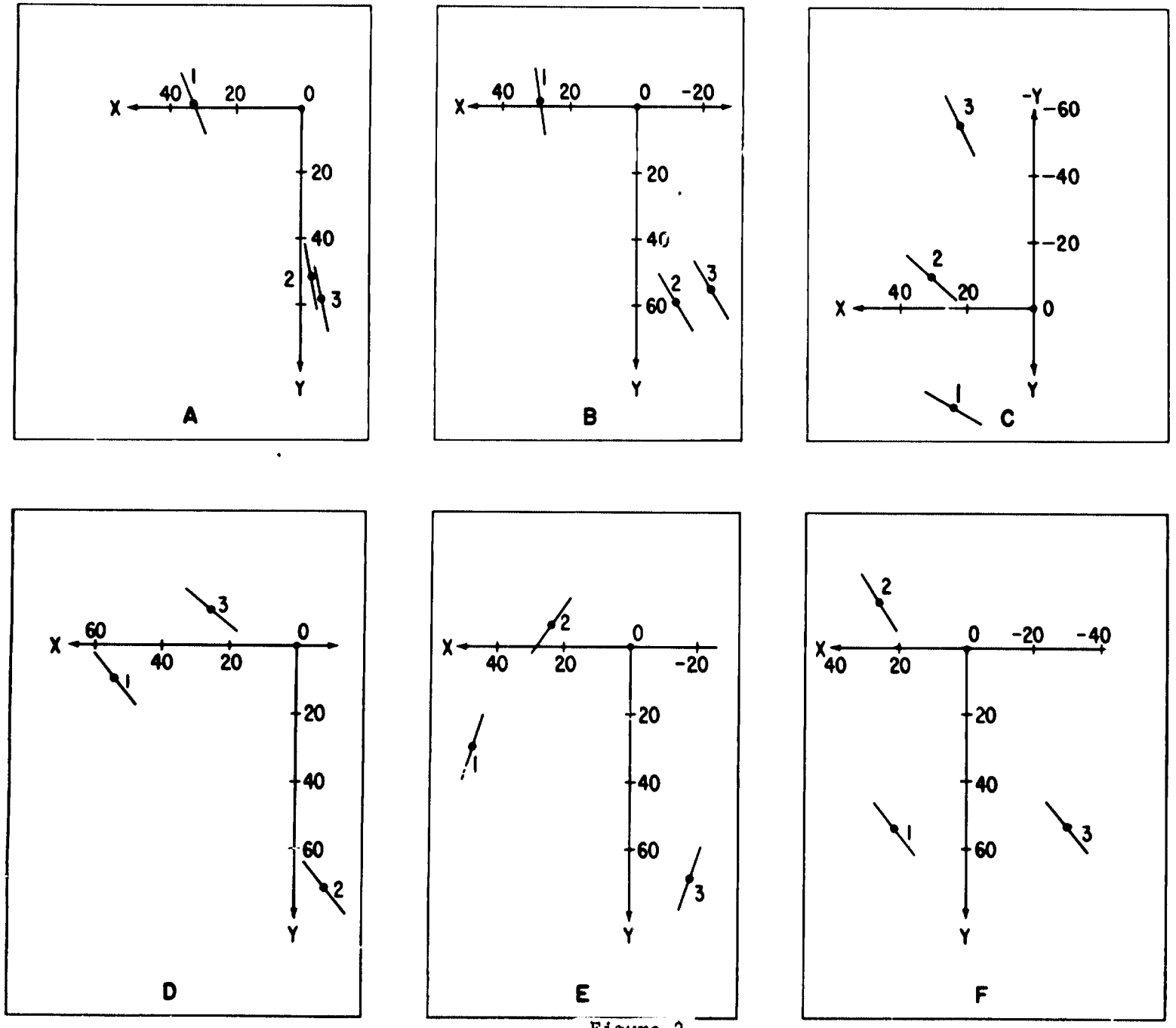
X
40
20
0
1
20
40
2
3
Y
A
X
40
20
0
-20
1
20
40
60
2
3
Y
B
-Y
-60
-40
-20
3
2
40
20
X
0
Y
1
C
X
60
40
20
0
3
1
20
40
60
2
Y
D
X
40
20
0
-20
2
1
20
40
60
3
Y
E
X
40
20
0
-20
-40
2
20
40
1
60
3
Y
F

Figure 2

TABLE I

	$\hat{n}_T$	$\hat{P}_{12}$	$\hat{P}_{13}$	$\cos^{-1}(\hat{P}_{12}\cdot\hat{P}_{13})$	t_{12}(min)	t_{13}(min)
A	$\begin{matrix}+.02 & +.12 & +.15\\ (.92 & .24 & .26)\\ -.02 & -.7 & -.18\end{matrix}$	(-.34, .92, .18)	(-.25, .97, -.01)	14°	5.5±.7	8.0±.7
B	$\begin{matrix}+.02 & +.11 & +.05\\ (.79 & .33 & -.48)\\ -.03 & -.20 & -.08\end{matrix}$	(-.42, .89, -.03)	(-.48, .86, -.13)	14°	3.8±2.3	6.8±1.6
C	$\begin{matrix}+.20 & +.16 & +.31\\ (+.67 & +.65 & -.06)\\ -.18 & -.23 & -.26\end{matrix}$	(.87, -.46, -.15)	(.78, -.62, -.04)	14°	15.1±.7	21.8±1.1
D	$\begin{matrix}+.03 & +.12 & +.07\\ (+.49 & +.44 & +.74)\\ -.06 & -.09 & -.05\end{matrix}$	(-.46, .85, -.22)	(.74, -.71, .11)	165°	7.0±1.4	11.6±1.2
E	$\begin{matrix}+.09 & +.09 & +.24\\ (+.86 & -.38 & -.20)\\ -.05 & -.18 & -.28\end{matrix}$	(-.34, -.93, -.11)	(.22, .87, -.43)	146°	3.2±.7	20.5±1.2
F	$\begin{matrix}+.19 & +.03 & +.22\\ (.63 & .46 & -.55)\\ -.11 & -.05 & -.19\end{matrix}$	(.47, -.86, .10)	(-.57, -.05, -.82)	108°	8.7±.7	10.0±1.3

	ϕ_{n_T}	θ_{n_T}	α_{12}	α_{13}	$\Delta\alpha$
A	15°	15°	93°	90°	±5°
B	23°	−26°	91°	92°	±8°
C	44°	3°	73°	83°	±12°
D	42°	−37°	91°	83°	±6°
E	−24°	1[illegible]°	85°	92°	±8°
F	36°	−29°	99°	86°	±9°
		Average	89°	88°	±8°

Table II

TABLE III
Current Sheets

Discontinuity	Thickness ($\times 10^{+8}$ cm)	Average $B_T \cdot \hat{n}$ (γ)	Remarks
A	3	$.05 \pm .1$	uniform rotation
B	~ 20	$\approx 1 \pm 1$	broad; erratic rotation
C	~ 2	$.5 \pm 1.0$	
D	8	$.1 \pm .3$	non-uniform rotation
E	$< .8$	—	too thin to be studied
F	1.8	$-.2 \pm .2$	

ACKNOWLEDGEMENTS

The authors wish to thank Dr. K. W. Ogilvie for providing bulk speed measurements from his experiment on Explorer 34, and for critically examining the manuscript. Helpful discussions with Dr. Y. C. Whang are also appreciated.